FRONTIERS OF PHYSICS

RESEARCH ARTICLE
Volume 18 / Issue 6 / 61301 / 2023

Preparing quantum states by measurement-feedback control with Bayesian optimization

Yadong Wu[1,2,3,4], Juan Yao[5,6,7], Pengfei Zhang[1,8,†]

1 Department of Physics, Fudan University, Shanghai 200438, China
2 State Key Laboratory of Surface Physics, Key Laboratory of Micro and Nano Photonic Structures (MOE), Fudan University, Shanghai 200438, China
3 Institute for Nanoelectronic Devices and Quantum Computing, Fudan University, Shanghai 200433, China
4 Shanghai Qi Zhi Institute, AI Tower, Xuhui District, Shanghai 200232, China
5 Shenzhen Institute for Quantum Science and Engineering, Southern University of Science and Technology, Shenzhen 518055, China
6 International Quantum Academy, Shenzhen 518048, China
7 Guangdong Provincial Key Laboratory of Quantum Science and Engineering, Southern University of Science and Technology, Shenzhen 518055, China
8 Walter Burke Institute for Theoretical Physics & Institute for Quantum Information and Matter, California Institute of Technology, Pasadena, CA 91125, USA
Corresponding author. E-mail: †pengfeizhang.physics@gmail.com
Received April 14, 2023; accepted May 24, 2023

ABSTRACT

The preparation of quantum states is crucial for enabling quantum computations and simulations. In this work, we present a general framework for preparing ground states of many-body systems by combining the measurement-feedback control process (MFCP) with machine learning techniques. Specifically, we employ Bayesian optimization (BO) to enhance the efficiency of determining the measurement and feedback operators within the MFCP. As an illustration, we study the ground state preparation of the one-dimensional Bose–Hubbard model. Through BO, we are able to identify optimal parameters that can effectively drive the system towards low-energy states with a high probability across various quantum trajectories. Our results open up new directions for further exploration and development of advanced control strategies for quantum computations and simulations.

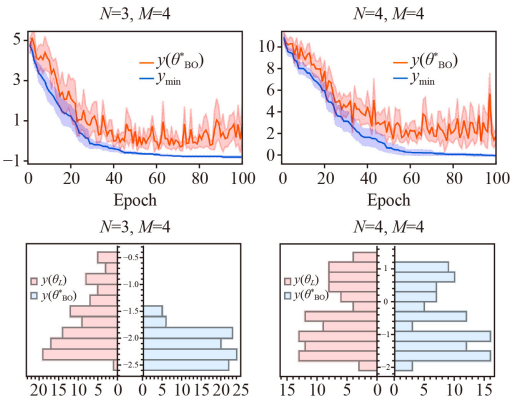

Keywords state preparation, feedback control, Bayesian optimization

1 Introduction

Quantum states preparation is an essential part of the research in the quantum physics field. Recently, it has been realized that measurements play an important role in preparing quantum states [1–13]. For states that can be specified by a set of stabilizers, including both the Greenberger–Horne–Zeilinger "cat" state and the toric code state, efficient preparation algorithms have been proposed by measuring cluster states and applying local unitary gates based on the measurement outcome [14–23]. This is an example of the measurement feedback control process (MFCP), where we measure the quantum system during the evolution of a quantum trajectory, obtain the measurement signal with random noise, and provide feedback controls to the quantum system based

https://doi.org/10.1007/s11467-023-1311-5

on measurement outcomes [24, 25]. MFCP is a valuable approach to affect the quantum system in a partially human-controlled way and has been wildly adopted in cold atoms, ion traps, photon cavities, and other systems [26–38].

Motivated by these developments, we explore the possibility of preparing more general ground states of lattice Hamiltonians using MFCP. We focus on MFCP with continuous weak measurements, for which concrete realization has been proposed in cold atom systems [39, 40]. Since the measurement signal is a random variable with a large variance because of the uncertainty principle, we get an ensemble of quantum trajectories instead of a single quantum state [41]. The protocol succeed only if typical quantum trajectories, instead of the averaged density matrix, have high fidelity with respect to the target. However, the MFCP contains much arbitrariness: Generally, it is not clear how to choose suitable measurement and feedback control operators to achieve the target state.

In this work, we utilize the machine learning (ML) method to overcome this difficulty and achieve high fidelity of preparing target states. There are many beautiful works on using ML in physics, including classifying different quantum phases, accelerating computation, preparing physical systems, and optimizing experimental control processes [42–76]. Among different ML algorithms, Bayesian optimization (BO) [77] stands out for obtaining the global maximum or minimum of a "black-box" function where the function form is complicated but unknown. It's usually applied in a situation where the label of the function is expensive to obtain or the dataset is not abundant, such as parameters control and experimental calibration [78–85]. We take the one-dimensional Bose–Hubbard model as an example and use BO to find the suitable measurement and feedback control operators for the ground-state preparation. After training, the MFCP can evolve the quantum system to states with low energy expectations, which are quite close to the true ground state.

2 Method

2.1 Measurement feedback control process

For systems evolved under the MFCP, we can divide the evolution time into a sequence of the interval length δt. At each time step, the evolution is composed of a weak measurement and an unitary evolution with feedback control Fig. 1(a). The weak measurement is described by a set of Kraus operators with $\{\hat{A}(\alpha)\}$ with $\alpha \in \mathbb{R}$, which are chosen to be a Gaussian function of a Hermitian measurement operator $\hat{c}$ [86]:

$$\hat{A}(\alpha) = \left(\frac{4\gamma\delta t}{\pi}\right)^{1/4} \mathrm{e}^{-2\gamma\delta t(\hat{c}-\alpha)^2}. \tag{1}$$

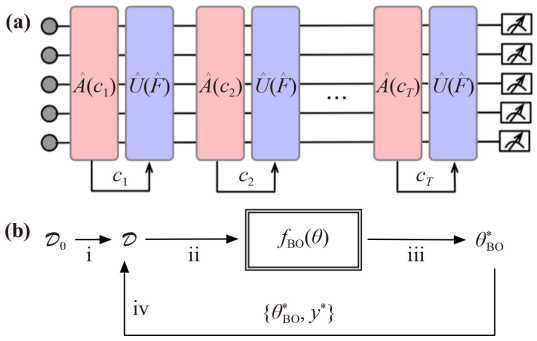

Fig. 1 **(a)** MFCP for a quantum system. $\hat{A}(c_m)$ is the measurement step and $\hat{U}(\hat{F})$ is the feedback control step. At each time interval, the feedback control step evolves the system with the measurement signal c_m. After T times the system is detected. **(b)** The general procedure of the BO method to obtain the global extremum of a "black-box" function $f(\theta)$.

Here γ is the dissipative strength and α is the measurement result. The normalization factor is chosen to satisfy $\int_{-\infty}^{\infty} \mathrm{d}\alpha\, \hat{A}(\alpha)^\dagger \hat{A}(\alpha) = \hat{I}$. Given a state $|\psi\rangle$, during each time interval, measurement result c_m satisfies the normal distribution $P(c_m) = \langle \hat{A}(c_m)^\dagger \hat{A}(c_m)\rangle \sim \mathcal{N}(\mu = \langle c\rangle, \sigma^2 = 1/(8\gamma)\delta t)$, where $\langle\cdots\rangle$ is taken under the state $|\psi\rangle$. Introducing the measurement signal δW, the measurement result can be rewritten as $c_m = \langle\hat{c}\rangle + \frac{\delta W}{\sqrt{8\gamma\delta t}}$, where the measurement signal $\delta W \sim \mathcal{N}(0, \delta t)$ represents the random noises in each weak measurement. After each weak measurement, the normalized quantum state evolves according to

$$\mathcal{M}_t|\psi(t)\rangle = \frac{1}{N}\mathrm{e}^{-2\gamma(\hat{c}-\langle\hat{c}\rangle)^2\delta t + \sqrt{2\gamma}(\hat{c}-\langle\hat{c}\rangle)\delta W}|\psi(t)\rangle, \tag{2}$$

which takes the form of an imaginary-time evolution with self-consistent field $\langle\hat{c}\rangle$ and random field δW. Here $1/N$ is the normalizing factor.

A feedback step is followed in order to control the system. We applying the Markovian feedback control to the system with a feedback term proportional to the measurement signal c_m added to the system. The unitary dynamic is described by

$$U_t|\psi(t)\rangle = \mathrm{e}^{-\mathrm{i}(\hat{H}_0 + c_m\hat{F})\delta t/\hbar}|\psi(t)\rangle, \tag{3}$$

where $\hat{F}$ is the feedback operator and $\hat{H}_0$ is the system Hamiltonian. Weak measurement [Eq. (2)] and feedback step [Eq. (3)] together constitute one loop of the dynamic evolution:

$$|\psi(t+\delta t)\rangle = U_t\mathcal{M}_t|\psi(t)\rangle. \tag{4}$$

As shown in Fig. 1(a), repeating the measurement-dependent feedback loop multiple times, the system is evolved to $|\psi(T)\rangle$.

The measurement-dependent feedback control can be used to tailor the system's dynamics and states. Proper

choice of measurement operator $\hat{c}$ and feedback operator $\hat{F}$ can lead to high fidelity between the evolved state $|\psi(T)\rangle$ and some target state such as the ground state $|\psi_g\rangle$ of some Hamiltonian. In most cases, the explicit form of the ground state is unknown and fidelity between the two states is unavailable. Alternative target functions such as state energy or entropy can be used to guide the choice of $\hat{c}$ and $\hat{F}$. Thus the key problem lies in how to determine the form of $\hat{c}$ and $\hat{F}$ which optimize the target function. In this work, we choose some operator basis and parameterize both $\hat{c}$ and $\hat{F}$ by their expansion coefficients α_j and β_j. In the following, we will adopt the machine learning method to determine the optimized parameters $\theta = \{\alpha_j, \beta_j\}$ for this measurement-dependent feedback control problem.

2.2 Bayesian optimization

Bayesian optimization (BO) is a strategy for global optimization. The ultimate goal of the BO method is to search for the extremum point of a black-box function $f(\theta)$. In order to simulate the relation between variables θ and $y = f(\theta)$, sampling of training dataset with $\mathcal{D} = \{(\theta_i, y_i)|i = 1, \cdots\}$ are required. In some cases, the label y of the function is hard to obtain. For example, it may require conducting a time consuming experiment for each parameter θ. BO method queries the labels online in an economical way and extends the training dataset through a small training dataset $\mathcal{D}_0$. It can obtain the global extremum with a limited number of labels which saves a significant amount of time and resources.

The general procedure of the BO method is summarized in Fig. 1(b). i) Initially, a small training dataset $\mathcal{D} = \mathcal{D}_0 = \{(\theta_i, y_i)|i = 1, \cdots, n_0)\}$ is prepared. ii) Train the BO model with the dataset $\mathcal{D}$ and obtain the approximated model $f_{\rm BO}(\theta)$. iii) Search for the extremum point $\theta^*_{\rm BO}$ of the training BO model $f_{\rm BO}(\theta)$. iv) Query the true label $y* = f(\theta^*_{\rm BO})$ and update the training dataset $\mathcal{D}$ by adding the new sample point $(\theta^*_{\rm BO}, y^*)$. Repeat steps ii)–iv) until the prediction is converged. Then we can claim that the BO optimization approaches the extremum point of the function $y^* = f(\theta^*)$. Although the training dataset is extended during the training process, it is possible that the limited number of training data points is not large enough to simulate the real function $f(\theta)$ in entire regimes. Nevertheless, the simulated $f_{\rm BO}$ is accurate enough to predict the extremum point of the $f(\theta)$ due to the query strategy adopted by the BO method.

In our setup, we are mainly interested in preparing ground states for lattice Hamiltonians. Compared to use fidelity as the target function, the energy is more realistic to be measured in experiments. As a result, we set the target function as the energy expectation values with $f(\theta) \equiv \langle\psi(T)|\hat{H}|\psi(T)\rangle$. For states with long-range orders at zero temperature, the correlation length of order parameters may also be used as the target function. Due to the stochastic property of the measurement result and the associated feedback control process, for each set of θ, each run of the dynamic evolution is only one of the many possible quantum trajectories. Considering the real experimental operation condition, we repeat the dynamic evolution 50 times and only take the first 25 quantum trajectories with minimal energy expectation values. Then for each set of parameters θ, $\overline{(\cdot)}$ corresponds to the average of the 25 quantum trajectories. All training processes are implemented in MATLAB Bayesian optimization toolbox.

Analytical Benchmark. Before turning to the example, we provide an analytical benchmark for our BO based protocol. Up to the fisrt order of δt, the MFCP is reduced to the stochastic master equation [25],

$$\mathrm{d}\hat{\rho} = -\mathrm{i}[\hat{H}_0 + \hat{H}_{\rm fb}, \hat{\rho}]\mathrm{d}t + \mathcal{D}[\hat{L}]\hat{\rho}\mathrm{d}t + \mathcal{H}[\hat{L}]\hat{\rho}\mathrm{d}W, \tag{5}$$

where $\mathcal{D}[\hat{L}]\hat{\rho} = \hat{L}\hat{\rho}\hat{L}^\dagger - \frac{1}{2}(\hat{L}^\dagger\hat{L}\hat{\rho} + \hat{\rho}\hat{L}^\dagger\hat{L}), \mathcal{H}[\hat{L}]\hat{\rho} = \hat{L}\hat{\rho} + \hat{\rho}\hat{L}^\dagger - \mathrm{Tr}[(\hat{L} + \hat{L}^\dagger)\hat{\rho}]\hat{\rho}$. $\hat{L} = (\sqrt{\gamma}\hat{c} - \mathrm{i}\hat{F})$ is the modified dissipation operator and $\hat{H}_{\rm fb} = \sqrt{\gamma}(\hat{c}^\dagger\hat{F} + \hat{F}\hat{c})$ is the modified feedback control Hamiltonian. After taking the ensemble average of Eq. (5) with $E[\mathrm{d}W] = 0$, the reduced master equation has a pure steady state which is the common eigenstate of $\hat{L}$ and $\hat{H}_{\rm eff} = \hat{H}_0 + \hat{H}_{\rm fb} - \mathrm{i}\hat{L}^\dagger\hat{L}/2$. As a result, by requiring the ground state as the steady state, i.e., $\hat{L}|\psi_g\rangle = 0$, it is possible to reach a steady state very close to the ground state $|\psi_g\rangle$ of $\hat{H}_0$ when the feedback control Hamiltonian $\hat{H}_{\rm fb}$ can be neglected for the weak measurement with strength $\gamma \sim 0$. Given the ground state $|\psi_g\rangle$, it is efficient to minimize the expectation value of $\langle\hat{L}^\dagger\hat{L}\rangle = \mathrm{Tr}[\hat{L}^\dagger\hat{L}|\psi_g\rangle\langle\psi_g|]/\mathrm{Tr}[\hat{L}^\dagger\hat{L}]$. This minimization procedure is equivalent to search the eigenvector with minimal eigenvalue of a semi-positive matrix $\mathcal{K}$. Here the element of the matrix is $\mathcal{K}_{lm} = \langle\psi_g|\hat{O}^\dagger_l\hat{O}_m|\psi_g\rangle$ with $\hat{O}_i$ as the operator basis for parametrization of $\hat{L}$, which is known as a correlation matrix [87–91]. The corresponding eigenvector with the minimal eigenvalue provides the expansion coefficients $\theta_{\rm L}$ with associated $\hat{L}_{\mathcal{K}}$, which can drive the system close to the ground state of $\hat{H}_0$. For the example discussed in the following, the ground state $|\psi_g\rangle$ is obtained numerically with exact diagonalization method.

3 Example

Now we present an example of our protocol using the Bose–Hubbard model. MFCP has been applied to prepare both the ground state and excited states in Ref. [92], where measurement and feedback operators are constructed based on the perturbative analysis in the non-interacting case. As a consequence, the performance decreases as the interaction strength increases. In the following, we take the Bose–Hubbard model as an example to illustrate how to determine the measurement and feedback operator with the BO method. Considering N

bosonic particles in a one-dimensional optical lattice of M sites. The Hamiltonian reads

$$\hat{H}_0 = -J\sum_{j}^{M-1}(\hat{a}_j^\dagger\hat{a}_{j+1} + \hat{a}_{j+1}^\dagger\hat{a}_j) + \frac{U}{2}\sum_{j}^{M}\hat{n}_j(\hat{n}_j - 1), \tag{6}$$

where J is the nearest-neighbor hopping strength, U is the contact interaction strength. Here $\hat{a}_j$ is the bosonic annihilation operator at the j_{th} site and $\hat{n}_j = \hat{a}_j^\dagger\hat{a}_j$ is the particle number operator. For experimental convenience, the measurement operator is set as the linear combination of the single-site particle number operators

$$\hat{c} = \sum_{j}^{M}\alpha_j\hat{n}_j, \tag{7}$$

and the feedback operator is proportional to the nearest neighbor hopping with

$$\hat{F} = (\beta_1 + \mathrm{i}\beta_2)\sum_{j}^{M-1}\hat{a}_j^\dagger\hat{a}_{j+1} + \mathrm{H.C.}, \tag{8}$$

where an overall modification of the hopping amplitude and phase is applied to the system. Realization of the scheme for the measurement operator $\hat{c}$ has been discussed in Refs. [93–95]. The feedback operator $\hat{F}$ can also be implemented by using photon-assisted hopping [25]. Then the coefficients $\theta = \{\alpha_j,\ \beta_1,\ \beta_2 | j = 1, ..., M\}$ will determine the final state of MFCP $|\psi(T)\rangle$. The same operator basis will also be used for the analytic benchmark analysis.

3.1 Non-interacting case

In this part, we apply the BO training process to the MFCP in the non-interaction regime with $U = 0$. We aim to search for the optimal parameters θ^* which determine the formalism of the measurement and feedback operators with a limited number of repeated dynamic evolution processes. We choose the hopping strength $J = 1$ as the energy unit. We set the dissipation strength $\gamma = 0.1$ and the time interval $\delta t = 0.1$. The total evolution time $\gamma T = 5$ is chosen to be long enough for the system to evolve to the target state. During the training process, we restrict all the parameters to $\theta \in (-5, 5)$. Initially, n_0 set of random sample points are provided with $D_0 = \{(\theta_i, y_i)|i = 1, \cdots, n_0 = 10)\}$. Due to the long time evolution, the initial state dependence is negligible. Each label $y_i = y(\theta_i)$ is the average of first 25 quantum trajectories with minimal energy expectation over 50 stochastic dynamic evolutions. During the BO training process, training dataset is extended by candidate optimal datapoint $\{\theta^*_{\mathrm{BO}}, y^*\}$ in each iterative loop or epoch as shown in Fig. 1(b).

For $M = 4$ and total number of particles $N = 3$ with fractional filling, we plot the energy $y(\theta^*_{\mathrm{BO}})$ of the candidate datapoint generated by the BO model in Fig. 2(a). As shown by the red dashed line, each line is the average of 10 independent training process. The shaded region around the red dashed lines stands for the variance of the independent training process. Taking into account of all the data points in the training dataset, the minimal energy y_{min} is plotted by the blue line in Fig. 2(a) where similar average of the training process is applied. It can be found that the variance of the minimal energy y_{min} decreases with large training epochs. The system converges into the ground state energy (the dotted line) with high probability. After training, BO method provides the optimal parameters θ^* and the associated measurement and feedback operator can drive the system to the ground state. As shown in Fig. 2(c), the blue solid line presented the state energy E_{BO} upon average of 20 different initial states. Analytically, in the non-interaction regime, numerical diagonalization of the semi-positive matrix $\mathcal{K}$ provides two zero eigenvalues. A combination of the two corresponding eigenvectors, which guarantees $\beta_1 = 0$ for the corresponding feedback operators, is chosen as the optimal coefficients θ_{L}. The corresponding dynamic evolution $y(\theta_{\mathrm{L}})$ is plotted in Fig.

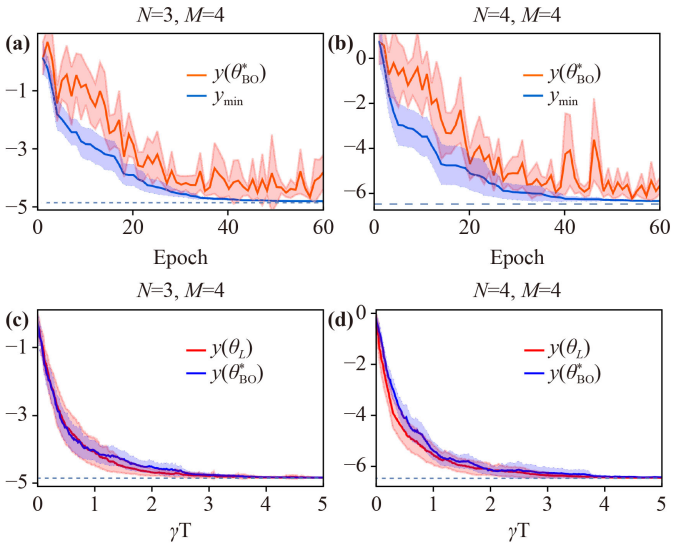

Fig. 2 **(a, b)** Energy expectation of non-interacting Hamiltonian. Red curves are the mean value of $y(\theta^*_{\mathrm{BO}})$ for each epoch. Blue curves are the mean value of the minimal energy expectation y_{min} during training. The shades are the minimal energy expectation standard variance of 10 different training processes. **(c, d)** Energy expectation during MFCP with 20 different initial states. Red curves are the mean value of energy expectation driven by analytical optimal operators with parameters θ_L. Red shades are the energy standard variance. Blue curves are the mean value of energy expectation driven by operators after BO training θ_{BO}. Gray dashed lines are the ground state energies without interaction. The true ground state energy is calculated as $E_0/J = -4.854$ for $N = 3, M = 4$ and $E_0/J = -6.472$ for $N = 4, M = 4$ respectively.

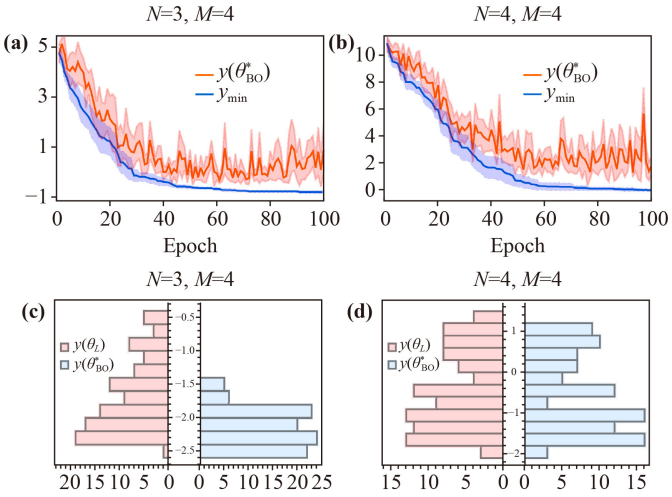

Fig. 3 **(a, b)** Energy expectation of strong interaction system. Red curves are the mean value of $E_{\mathrm{BO}} = y(\theta^*_{\mathrm{BO}})$ for each epoch. Blue curves are the mean value of the minimal energy expectation E_{min} during training. The shades are the minimal energy expectation standard variance of 10 different training processes. With strong interactions, true ground state energy is calculated as $E_0/J = -2.771$ for $N = 3, M = 4$ and $E_0/J = -2.204$ for $N = 4, M = 4$. **(c, d)** Histogram of the first 100 small state energy among 200 dynamic trajectories. The light-red bar denotes the MFCP driven by θ_L and the light-blue bar denotes the MFCP driven by θ_{BO}.

2(c) which provides an analytic benchmark for our BO strategy for the MFCP. The result indicates that the parameters learnt by the BO strategy indeed guide the system to the ground state as well as the benchmark. For integer filling with $M = N = 4$, similar results are also presented in Figs. 2(b) and (d).

3.2 Strongly interacting case

Here we set the interaction strength $U/J = 5$. Figures 3(a) and (b) show the BO training results for both fractional and integer filling. It can be found that energy expectations $y(\theta^*_{\mathrm{BO}})$ (red lines) have large fluctuations even the minimal energy (blue lines) expectations are converged. Compared to the non-interacting case, it is much harder to reach the ground state energy. In this situation, analytically the eigenvalues of the matrix $\mathcal{K}$ are all positive. The eigenvector for the minimal eigenvalue is chosen with $\langle \hat{L}^\dagger_{\mathcal{K}} \hat{L}_{\mathcal{K}} \rangle = 0.0025$ and 0.001 for the fractional and integer filling respectively. For the parameters learnt by the BO method, the corresponding $\langle \hat{L}^\dagger_{\mathrm{BO}} \hat{L}_{\mathrm{BO}} \rangle$ is calculated as 0.005 and 0.0004 respectively which is the same order of the analytic benchmark result. The deviation of $\langle \hat{L}^\dagger \hat{L} \rangle$ from zero is possibly due to the incompleteness of the operator basis. For practical analysis provided by the optimal parameters θ, we conduct the dynamic evolution for the measurement and feedback process to the final state for 200 times and plot the first 100 trajectories with minimal energy in Figs. 3(c) and (d). The histogram of the distribution of the state energy indicates a larger occupation of the low energy state with the parameters θ_{BO} provided by BO method compared to θ_{L} by the analytic benchmark. Namely, adopting the parameters provided by the BO method has a larger probability to drive the system to the target state.

4 Discussion

In this work, we use machine learning method, Bayesian optimization (BO), to optimize the operators for the measurement and feedback process to drive the system to a target state. Taking the one dimensional Bose-Hubbard model as an example, we show that BO can give us a parameter set to drive systems to the low energy state for a given operator basis. Our discussions provide a general scheme for optimizing the controlling parameters, including preparing different classes of target states beyond ground states. Applying this machine learning method only asks for these conditions. First, the entire control process can be quantified. All parameters θ can be quantitatively determined and can be digitally described. Then once these parameters are fixed, the label $y(\theta)$ is also determined and repeatable. The mapping between parameters and labels can be complicated, and querying labels would be at an expensive cost. Our scheme is also model free. We do not need to design a specific machine learning scheme for every optimization task.

We can consider a number of generalizations of such studies. Firstly, it is interesting to reveal the supremacy of our protocol in quantum simulation and quantum computation, such as infault-tolerant quantum computations [96–99]. Secondly, our state preparation method could be further improved on gate-model quantum computers [100–103]. For instance, one could employ an efficient measurement strategy to reduce the number of required measurement rounds for determining the system energy [101]. Additionally, conducting a comparison between our method and previous proposals for state preparation would be beneficial [100]. Then, there still exist many open questions in quantum dynamical phase transition in open systems and some dissipative-driven phase transition [104–106]. So MFCP with ML may provide new ways to realize novel forms of dissipative criticality. What's more, recent research indicates that measurements would induce a new kind of phase transition in open systems [107–110], which means that the measurement-feedback control process also has some critical properties.

Conflicts of interest There are no conflicts to declare.

Acknowledgements Y.W. is supported by the National Program on Key Basic Research Project of China (Grant No. 2021YFA1400900)

and the National Natural Science Foundation of China (Grant No. 12174236). P.Z. is partly supported by the Walter Burke Institute for Theoretical Physics at Caltech. J.Y. is supported by the National Natural Science Foundation of China (Grant No. 11904190) and Guangdong Basic and Applied Basic Research Foundation (Grant No. 2022B1515120021).

References

1. J. M. Geremia, J. K. Stockton, and H. Mabuchi, Real-time quantum feedback control of atomic spin-squeezing, *Science* 304(5668), 270 (2004)
2. J. M. Geremia, Deterministic and nondestructively verifiable preparation of photon number states, *Phys. Rev. Lett.* 97(7), 073601 (2006)
3. M. Yanagisawa, Quantum feedback control for deterministic entangled photon generation, *Phys. Rev. Lett.* 97(19), 190201 (2006)
4. A. Negretti, U. V. Poulsen, and K. Mølmer, Quantum superposition state production by continuous observations and feedback, *Phys. Rev. Lett.* 99(22), 223601 (2007)
5. C. Sayrin, I. Dotsenko, X. Zhou, B. Peaudecerf, T. Rybarczyk, S. Gleyzes, P. Rouchon, M. Mirrahimi, H. Amini, M. Brune, J. M. Raimond, and S. Haroche, Real-time quantum feedback prepares and stabilizes photon number states, *Nature* 477(7362), 73 (2011)
6. X. Zhou, I. Dotsenko, B. Peaudecerf, T. Rybarczyk, C. Sayrin, S. Gleyzes, J. M. Raimond, M. Brune, and S. Haroche, Field locked to a Fock state by quantum feedback with single photon corrections, *Phys. Rev. Lett.* 108(24), 243602 (2012)
7. D. Ristè, M. Dukalski, C. A. Watson, G. de Lange, M. J. Tiggelman, Ya. M. Blanter, K. W. Lehnert, R. N. Schouten, and L. DiCarlo, Deterministic entanglement of superconducting qubits by parity measurement and feedback, *Nature* 502(7471), 350 (2013)
8. R. Inoue, S. I. R. Tanaka, R. Namiki, T. Sagawa, and Y. Takahashi, Unconditional quantumnoise suppression via measurement-based quantum feedback, *Phys. Rev. Lett.* 110(16), 163602 (2013)
9. A. C. J. Wade, J. F. Sherson, and K. Mølmer, Squeezing and entanglement of density oscillations in a Bose-Einstein condensate, *Phys. Rev. Lett.* 115(6), 060401 (2015)
10. K. C. Cox, G. P. Greve, J. M. Weiner, and J. K. Thompson, Deterministic squeezed states with collective measurements and feedback, *Phys. Rev. Lett.* 116(9), 093602 (2016)
11. M. Gajdacz, A. J. Hilliard, M. A. Kristensen, P. L. Pedersen, C. Klempt, J. J. Arlt, and J. F. Sherson, Preparation of ultracold atom clouds at the shot noise level, *Phys. Rev. Lett.* 117(7), 073604 (2016)
12. J. Lammers, H. Weimer, and K. Hammerer, Open-system many-body dynamics through interferometric measurements and feedback, *Phys. Rev. A* 94(5), 052120 (2016)
13. V. Sudhir, D. J. Wilson, R. Schilling, H. Schütz, S. A. Fedorov, A. H. Ghadimi, A. Nunnenkamp, and T. J. Kippenberg, Appearance and disappearance of quantum correlations in measurement-based feedback control of a mechanical oscillator, *Phys. Rev. X* 7(1), 011001 (2017)
14. H. J. Briegel and R. Raussendorf, 0, Persistent entanglement in arrays of interacting particles, *Phys. Rev. Lett.* 86(5), 910 (2001)
15. R. Raussendorf, S. Bravyi, and J. Harrington, Long-range quantum entanglement in noisy cluster states, *Phys. Rev. A* 71(6), 062313 (2005)
16. R. Verresen, N. Tantivasadakarn, and A. Vishwanath, Efficiently preparing Schrödinger's cat, fractons and non-Abelian topological order in quantum devices, arXiv: 2112.03061 (2021)
17. N. Tantivasadakarn, R. Thorngren, A. Vishwanath, and R. Verresen, Long-range entanglement from measuring symmetry-protected topological phases, arXiv: 2112.01519 (2021)
18. G. Y. Zhu, N. Tantivasadakarn, A. Vishwanath, S. Trebst, and R. Verresen, Nishimori's cat: Stable long-range entanglement from finite-depth unitaries and weak measurements, arXiv: 2208.11136 (2022)
19. J. Y. Lee, W. Ji, Z. Bi, and M. Fisher, Measurement-prepared quantum criticality: From Ising model to gauge theory, and beyond, arXiv: 2208.11699 (2022)
20. N. Tantivasadakarn, A. Vishwanath, and R. Verresen, A hierarchy of topological order from finite depth unitaries, measurement and feedforward, arXiv: 2209.06202 (2022)
21. S. Bravyi, I. Kim, A. Kliesch, and R. Koenig, Adaptive constant-depth circuits for manipulating non-Abelian anyons, arXiv: 2205.01933 (2022)
22. T. C. Lu, L. A. Lessa, I. H. Kim, and T. H. Hsieh, Measurement as a shortcut to long-range entangled quantum matter, arXiv: 2206.13527 (2022)
23. S. Wu and Z. Cai, Feedback-induced interactive dynamics: Unitary but dissipative evolution, arxiv: 2211.09291 (2022)
24. H. M. Wiseman, Quantum theory of continuous feedback, *Phys. Rev. A* 49(3), 2133 (1994)
25. J. Zhang, Y. Liu, R. B. Wu, K. Jacobs, and F. Nori, Quantum feedback: Theory, experiments, and applications, *Phys. Rep.* 679, 1 (2017)
26. L. K. Thomsen, S. Mancini, and H. M. Wiseman, Spin squeezing via quantum feedback, *Phys. Rev. A* 65(6), 061801 (2002)
27. C. A. Muschik, K. Hammerer, E. S. Polzik, and I. J. Cirac, Quantum teleportation of dynamics and effective interactions between remote systems, *Phys. Rev. Lett.* 111(2), 020501 (2013)
28. A. L. Grimsmo, A. S. Parkins, and B. S. Skagerstam, Rapid steady-state convergence for quantum systems using time-delayed feedback control, *New J. Phys.* 16(6), 065004 (2014)
29. W. Kopylov, C. Emary, E. Schöll, and T. Brandes, Time-delayed feedback control of the Dicke–Hepp–Lieb superradiant quantum phase transition, *New J. Phys.* 17(1), 013040 (2015)
30. G. Mazzucchi, S. F. Caballero-Benitez, D. A. Ivanov, and I. B. Mekhov, Quantum optical feedback control for creating strong correlations in many-body systems, *Optica* 3(11), 1213 (2016)

31. A. Shankar, G. P. Greve, B. Wu, J. K. Thompson, and M. Holland, Continuous real-time tracking of a quantum phase below the standard quantum limit, *Phys. Rev. Lett.* 122(23), 233602 (2019)
32. D. A. Ivanov, T. Y. Ivanova, S. F. Caballero-Benitez, and I. B. Mekhov, Cavityless self-organization of ultracold atoms due to the feedback-induced phase transition, *Sci. Rep.* 10(1), 10550 (2020)
33. D. A. Ivanov, T. Yu. Ivanova, S. F. Caballero-Benitez, and I. B. Mekhov, Feedback-induced quantum phase transitions using weak measurements, *Phys. Rev. Lett.* 124(1), 010603 (2020)
34. K. Kroeger, N. Dogra, R. Rosa-Medina, M. Paluch, F. Ferri, T. Donner, and T. Esslinger, Continuous feedback on a quantum gas coupled to an optical cavity, *New J. Phys.* 22(3), 033020 (2020)
35. M. H. Muñoz-Arias, P. M. Poggi, P. S. Jessen, and I. H. Deutsch, Simulating nonlinear dynamics of collective spins via quantum measurement and feedback, *Phys. Rev. Lett.* 124(11), 110503 (2020)
36. M. H. Muñoz-Arias, I. H. Deutsch, P. S. Jessen, and P. M. Poggi, Simulation of the complex dynamics of mean-field p-spin models using measurement-based quantum feedback control, *Phys. Rev. A* 102(2), 022610 (2020)
37. H. M. Hurst, S. Guo, and I. B. Spielman, Feedback induced magnetic phases in binary Bose-Einstein condensates, *Phys. Rev. Res.* 2(4), 043325 (2020)
38. D. A. Ivanov, T. Yu. Ivanova, S. F. Caballero-Benitez, and I. B. Mekhov, Tuning the universality class of phase transitions by feedback: Open quantum systems beyond dissipation, *Phys. Rev. A* 104(3), 033719 (2021)
39. H. M. Hurst and I. B. Spielman, Measurement-induced dynamics and stabilization of spinor-condensate domain walls, *Phys. Rev. A* 99(5), 053612 (2019)
40. J. T. Young, A. V. Gorshkov, and I. B. Spielman, Feedback-stabilized dynamical steady states in the bosehubbard model, *Phys. Rev. Res.* 3(4), 043075 (2021)
41. H. M. Wiseman and G. J. Milburn, Quantum Measurement and Control, Cambridge University Press, 2009
42. H. Shen, J. Liu, and L. Fu, Self-learning Monte Carlo with deep neural networks, *Phys. Rev. B* 97(20), 205140 (2018)
43. C. Wang and H. Zhai, Machine learning of frustrated classical spin models (i): Principal component analysis, *Phys. Rev. B* 96(14), 144432 (2017)
44. P. Zhang, H. Shen, and H. Zhai, Machine learning topological invariants with neural networks, *Phys. Rev. Lett.* 120(6), 066401 (2018)
45. C. Wang and H. Zhai, Machine learning of frustrated classical spin models (ii): Kernel principal component analysis, *Front. Phys.* 13(5), 130507 (2018)
46. N. Sun, J. Yi, P. Zhang, H. Shen, and H. Zhai, Deep learning topological invariants of band insulators, *Phys. Rev. B* 98(8), 085402 (2018)
47. T. Song and H. Lee, Accelerated continuous time quantum Monte Carlo method with machine learning, *Phys. Rev. B* 100(4), 045153 (2019)
48. C. Wang, H. Zhai, and Y. Z. You, Emergent Schrödinger equation in an introspective machine learning architecture, *Sci. Bull. (Beijing)* 64(17), 1228 (2019)
49. Y. Zhang, A. Mesaros, K. Fujita, S. D. Edkins, M. H. Hamidian, K. Ch'ng, H. Eisaki, S. Uchida, J. C. S. Davis, E. Khatami, and E. A. Kim, Machine learning in electronic-quantum-matter imaging experiments, *Nature* 570(7762), 484 (2019)
50. B. S. Rem, N. Käming, M. Tarnowski, L. Asteria, N. Fläschner, C. Becker, K. Sengstock, and C. Weitenberg, Identifying quantum phase transitions using artificial neural networks on experimental data, *Nat. Phys.* 15(9), 917 (2019)
51. A. Bohrdt, C. S. Chiu, G. Ji, M. Xu, D. Greif, M. Greiner, E. Demler, F. Grusdt, and M. Knap, Classifying snapshots of the doped Hubbard model with machine learning, *Nat. Phys.* 15(9), 921 (2019)
52. J. Yao, Y. Wu, J. Koo, B. Yan, and H. Zhai, Active learning algorithm for computational physics, *Phys. Rev. Res.* 2(1), 013287 (2020)
53. G. Torlai, B. Timar, E. P. L. van Nieuwenburg, H. Levine, A. Omran, A. Keesling, H. Bernien, M. Greiner, V. Vuletić, M. D. Lukin, R. G. Melko, and M. Endres, Integrating neural networks with a quantum simulator for state reconstruction, *Phys. Rev. Lett.* 123(23), 230504 (2019)
54. A. M. Palmieri, E. Kovlakov, F. Bianchi, D. Yudin, S. Straupe, J. D. Biamonte, and S. Kulik, Experimental neural network enhanced quantum tomography, *npj Quantum Inf.* 6(1), 20 (2020)
55. Y. Wu, Z. Meng, K. Wen, C. Mi, J. Zhang, and H. Zhai, Active learning approach to optimization of experimental control, *Chin. Phys. Lett.* 37(10), 103201 (2020)
56. V. Saggio, B. E. Asenbeck, A. Hamann, T. Strömberg, P. Schiansky, V. Dunjko, N. Friis, N. C. Harris, M. Hochberg, D. Englund, S. Wölk, H. J. Briegel, and P. Walther, Experimental quantum speed-up in reinforcement learning agents, *Nature* 591(7849), 229 (2021)
57. Y. Baum, M. Amico, S. Howell, M. Hush, M. Liuzzi, P. Mundada, T. Merkh, A. R. R. Carvalho, and M. J. Biercuk, Seantal deep reinforcement learning for error-robust gate-set design on a superconducting quantum computer, *PRX Quantum* 2(4), 040324 (2021)
58. D. Castaldo, M. Rosa, and S. Corni, Quantum optimal control with quantum computers: A hybrid algorithm featuring machine learning optimization, *Phys. Rev. A* 103(2), 022613 (2021)
59. V. V. Sivak, A. Eickbusch, H. Liu, B. Royer, I. Tsioutsios, and M. H. Devoret, Model-free quantum control with reinforcement learning, *Phys. Rev. X* 12(1), 011059 (2022)
60. P. A. Erdman and F. Noé, Identifying optimal cycles in quantum thermal machines with reinforcement-learning, *npj Quantum Inf.* 8(1), 1 (2022)
61. M. F. Langer, A. Goeßmann, and M. Rupp, Representations of molecules and materials for interpolation of quantum-mechanical simulations via machine learning, *npj Comput. Mater.* 8(1), 41 (2022)
62. I. A. Luchnikov, E. O. Kiktenko, M. A. Gavreev, H. Ouerdane, S. N. Filippov, and A. K. Fedorov, Probing non-Markovian quantum dynamics with data-driven

analysis: Beyond "blackbox" machine-learning models, *Phys. Rev. Res.* 4(4), 043002 (2022)
63. I. Khait, J. Carrasquilla, and D. Segal, Optimal control of quantum thermal machines using machine learning, *Phys. Rev. Res.* 4(1), L012029 (2022)
64. J. Carrasquilla and R. G. Melko, Machine learning phases of matter, *Nat. Phys.* 13(5), 431 (2017)
65. E. P. L. van Nieuwenburg, Y. H. Liu, and S. D. Huber, Learning phase transitions by confusion, *Nat. Phys.* 13(5), 435 (2017)
66. Y. Zhang and E. A. Kim, Quantum loop topography for machine learning, *Phys. Rev. Lett.* 118(21), 216401 (2017)
67. D. L. Deng, X. Li, and S. Das Sarma, Machine learning topological states, *Phys. Rev. B* 96(19), 195145 (2017)
68. Y. H. Liu and E. P. L. van Nieuwenburg, Discriminative cooperative networks for detecting phase transitions, *Phys. Rev. Lett.* 120(17), 176401 (2018)
69. X. Y. Dong, F. Pollmann, and X. F. Zhang, Machine learning of quantum phase transitions, *Phys. Rev. B* 99(12), 121104 (2019)
70. G. Carleo and M. Troyer, Solving the quantum many-body problem with artificial neural networks, *Science* 355(6325), 602 (2017)
71. X. Gao and L. M. Duan, Efficient representation of quantum many-body states with deep neural networks, *Nat. Commun.* 8(1), 662 (2017)
72. Z. Cai and J. Liu, Approximating quantum many-body wave functions using artificial neural networks, *Phys. Rev. B* 97(3), 035116 (2018)
73. H. Saito, Method to solve quantum few-body problems with artificial neural networks, *J. Phys. Soc. Jpn.* 87(7), 074002 (2018)
74. G. Torlai, G. Mazzola, J. Carrasquilla, M. Troyer, R. Melko, and G. Carleo, Neuralnetwork quantum state tomography, *Nat. Phys.* 14(5), 447 (2018)
75. Y. Wu, P. Zhang, H. Shen, and H. Zhai, Visualizing a neural network that develops quantum perturbation theory, *Phys. Rev. A* 98(1), 010701 (2018)
76. C. Wang, H. Li, Z. Hao, X. Li, C. Zou, P. Cai, Y. Wang, Y. Z. You, and H. Zhai, Machine learning identification of impurities in the STM images, *Chin. Phys. B* 29(11), 116805 (2020)
77. B. Shahriari, K. Swersky, Z. Wang, R. P. Adams, and N. de Freitas, Taking the human out of the loop: A review of Bayesian optimization, *Proc. IEEE* 104(1), 148 (2016)
78. R. A. Vargas-Hernández, Y. Guan, D. H. Zhang, and R. V. Krems, Bayesian optimization for the inverse scattering problem in quantum reaction dynamics, *New J. Phys.* 21(2), 022001 (2019)
79. R. Mukherjee, F. Sauvage, H. Xie, R. Löw, and F. Mintert, Preparation of ordered states in ultra-cold gases using Bayesian optimization, *New J. Phys.* 22(7), 075001 (2020)
80. A. Kuroś, R. Mukherjee, W. Golletz, F. Sauvage, K. Giergiel, F. Mintert, and K. Sacha, Phase diagram and optimal control for n-tupling discrete time crystal, *New J. Phys.* 22(9), 095001 (2020)
81. F. Sauvage and F. Mintert, Optimal quantum control with poor statistics, *PRX Quantum* 1(2), 020322 (2020)
82. C. T. Belmiro Chu, Y. L. Sheu, and S. I. Chu, Bayesian optimal control of the ultrashort circularly polarized attosecond pulse generation by two-color polarization gating, *Opt. Express* 29(21), 32900 (2021)
83. A. Kuroś, R. Mukherjee, F. Mintert, and K. Sacha, Controlled preparation of phases in two-dimensional time crystals, *Phys. Rev. Res.* 3(4), 043203 (2021)
84. Y. J. Xie, H. N. Dai, Z. S. Yuan, Y. Deng, X. Li, Y. A. Chen, and J. W. Pan, Bayesian learning for optimal control of quantum many-body states in optical lattices, *Phys. Rev. A* 106(1), 013316 (2022)
85. C. L. Cortes, P. Lefebvre, N. Lauk, M. J. Davis, N. Sinclair, S. K. Gray, and D. Oblak, Sample-efficient adaptive calibration of quantum networks using Bayesian optimization, *Phys. Rev. Appl.* 17(3), 034067 (2022)
86. K. Jacobs and D. A. Steck, A straightforward introduction to continuous quantum measurement, *Contemp. Phys.* 47(5), 279 (2006)
87. X. L. Qi and D. Ranard, Determining a local Hamiltonian from a single eigenstate, *Quantum* 3, 159 (2019)
88. E. Bairey, I. Arad, and N. H. Lindner, Learning a local Hamiltonian from local measurements, *Phys. Rev. Lett.* 122(2), 020504 (2019)
89. E. Chertkov and B. K. Clark, Computational inverse method for constructing spaces of quantum models from wave functions, *Phys. Rev. X* 8(3), 031029 (2018)
90. Z. Li, L. Zou, and T. H. Hsieh, Hsieh. Hamiltonian tomography via quantum quench, *Phys. Rev. Lett.* 124(16), 160502 (2020)
91. Z. Yao, L. Pan, S. Liu, and P. Zhang, Bounding entanglement entropy using zeros of local correlation matrices, *Phys. Rev. Res.* 4(4), L042037 (2022)
92. L. N. Wu and A. Eckardt, Cooling and state preparation in an optical lattice via Markovian feedback control, *Phys. Rev. Res.* 4(2), L022045 (2022)
93. H. Ritsch, P. Domokos, F. Brennecke, and T. Esslinger, Cold atoms in cavity-generated dynamical optical potentials, *Rev. Mod. Phys.* 85(2), 553 (2013)
94. T. J. Elliott, W. Kozlowski, S. F. Caballero-Benitez, and I. B. Mekhov, Multipartite entangled spatial modes of ultracold atoms generated and controlled by quantum measurement, *Phys. Rev. Lett.* 114(11), 113604 (2015)
95. Y. Ashida and M. Ueda, Diffraction-unlimited position measurement of ultracold atoms in an optical lattice, *Phys. Rev. Lett.* 115(9), 095301 (2015)
96. P. W. Shor, Fault-tolerant quantum computation, in: Proceedings of 37th Conference on Foundations of Computer Science, pp 56–65, IEEE, 1996
97. D. Aharonov and M. Ben-Or, Fault-tolerant quantum computation with constant error, in: Proceedings of the Twenty-ninth Annual ACM Symposium on Theory of Computing, pp 176–188, 1997
98. J. Preskill, Fault-tolerant quantum computation, in: Introduction to Quantum Computation and Information, pp 213–269, World Scientific, 1998
99. D. Gottesman, Theory of fault-tolerant quantum computation, *Phys. Rev. A* 57(1), 127 (1998)
100. L. Gyongyosi, Quantum state optimization and

computational pathway evaluation for gate-model quantum computers, *Sci. Rep.* 10(1), 4543 (2020)

101. L. Gyongyosi and S. Imre, Dense quantum measurement theory, *Sci. Rep.* 9(1), 6755 (2019)
102. L. Gyongyosi and S. Imre, Training optimization for gate-model quantum neural networks, *Sci. Rep.* 9(1), 12679 (2019)
103. L. Gyongyosi and S. Imre, Advances in the quantum internet, *Commun. ACM* 65(8), 52 (2022)
104. E. G. D. Torre, S. Diehl, M. D. Lukin, S. Sachdev, and P. Strack, Keldysh approach for nonequilibrium phase transitions in quantum optics: Beyond the Dicke model in optical cavities, *Phys. Rev. A* 87(2), 023831 (2013)
105. M. F. Maghrebi and A. V. Gorshkov, Nonequilibrium many-body steady states via Keldysh formalism, *Phys. Rev. B* 93(1), 014307 (2016)
106. M. Foss-Feig, P. Niroula, J. T. Young, M. Hafezi, A. V. Gorshkov, R. M. Wilson, and M. F. Maghrebi, Emergent equilibrium in many-body optical bistability, *Phys. Rev. A* 95(4), 043826 (2017)
107. B. Skinner, J. Ruhman, and A. Nahum, Measurement-induced phase transitions in the dynamics of entanglement, *Phys. Rev. X* 9(3), 031009 (2019)
108. S. Choi, Y. Bao, X. L. Qi, and E. Altman, Quantum error correction in scrambling dynamics and measurement-induced phase transition, *Phys. Rev. Lett.* 125(3), 030505 (2020)
109. Q. Tang and W. Zhu, Measurement-induced phase transition: A case study in the nonintegrable model by density matrix renormalization group calculations, *Phys. Rev. Res.* 2(1), 013022 (2020)
110. R. Fan, S. Vijay, A. Vishwanath, and Y. Z. You, Self-organized error correction in random unitary circuits with measurement, *Phys. Rev. B* 103(17), 174309 (2021)